Biodiesel synthesis using clinoptilolite-Fe_3O_4-based phosphomolybdic acid as a novel magnetic green catalyst from *salvia mirzayanii* oil via electrolysis method: Optimization study by Taguchi method

Maryam Helmi[1], Mahdi Ghadiri[2*], Kambiz Tahvildari[3], Alireza Hemmati[4,*]

[1]Young Researchers and Elites club, Science and Research Branch, Islamic Azad University, Tehran, Iran

[2]Department of Chemical Engineering, University of Johannesburg, Doornfontein Campus 2028, Johannesburg, South Africa

[3]Department of chemistry, North Tehran Branch, Islamic Azad University, Tehran, Iran

[4] School of Chemical, Petroleum and Gas Engineering, Iran University of Science and Technology, Tehran, Iran

*Corresponding Authors's E-mail addresses: mahdig@uj.ac.za (M.Ghadiri), alireza_hemmati@iust.ac.ir (A.R. Hemmati),

Abstract:

Objective of current study is the synthesis of biodiesel from *salvia mirzayanii* oil using phosphomolybdic acid ($H_3PMo_{12}O_{40}$, HPA) supported on the clinoptilolite-Fe_3O_4. The prepared catalyst properties were determined by different analyses including FESEM, EDX, TEM, FTIR, and VSM, and its performance was studied in the process of biodiesel production. Four key factors effects like reaction time, catalyst weight, methanol to oil molar ratio, and temperature were investigated and optimized by the Taguchi method. In this method, the significance of effective factors on the biodiesel yield is controlled by analysis of variance (ANOVA). The highest biodiesel yield was found 80% at operating conditions of 0.5 wt.% HPA/clinoptilolite-Fe_3O_4 catalyst, methanol/oil ratio of 12:1, and temperature of 75 °C at 8 hours. The GC-MS analysis identified the fatty acid profile of *salvia mirzayanii* oil and biodiesel, the FTIR spectrum was performed to ensure biodiesel formation from the final product. The H-NMR analysis compared the properties of oil and biodiesel. The physicochemical properties of the produced biodiesel revealed that the biodiesel has the same properties as the diesel. Also, it can be deduced that the synthesized

biodiesel from *salvia mirzayanii* oil via electrolysis method is an economic and suitable method to produce biodiesel.

Keywords: Biodiesel; Electrolysis method; Magnetic solid catalyst; *Salvia mirzayanii*; Phosphomolybdic acid; Clinoptilolite;

1. Introduction

Reduction in fossil fuel sources, environmental pollution from combustion of fuel in engines, and concerns about energy supply have led researchers to look for renewable sources for the energy. Biodiesel is known as 'green fuel' and contains fatty acid methyl ester (FAME). It is eco-friendly and has high ignition, non-toxic, biodegradable properties to use as an alternative energy source [1]. Biodiesel has a high flash point (>130 °C), octane number, and high combustion yield and also an appropriate density and viscosity, excellent lubricant, and free sulfur and aromatic compounds [2]. These properties have been applied in the present engine without any modification and preheating.

Biodiesel is synthesized by the trans-esterification reaction of triglyceride oil such as non-edible or edible vegetable oils with alcohol using an appropriate catalyst that produces the fatty acid alkyl and glycerol [3]. Through that, most animal fats and vegetable oils are known as the sources of human feeding and usage of them for the biodiesel production is unjustified.

Non-edible oils such as *firmiana platanifolia L.f.* oil [4], *capparis spinosa* [5], *amygdalus scoparia* [6], virgin cottonseed oil [7], *euonymus maackii Rupr*. seed oil [8] and microalgal biomass [9] were studied as the source for the production of biodiesel. However, the sources of biodiesel production should be significantly available with properties of ease of access and growth in different climates based on the literature [10]. Iran has a warm and dry climate that most of its lands is desert. Therefore, the feedstock source of biodiesel production must be adapted to these conditions.

Salvia mirzayani as a wild-flowering plant is one of the *Salvia* (*Labiatae*) family that grows in tropical parts of Semnan and Khorasan-Razavi provinces, Iran [11]. Its height is 20-40 cm. It is a perennial biennial or herbaceous plant [12, 13]. This plant has been used in Iran as an

antimicrobial and antiviral agent due to its antioxidant properties [14] Figure. S1 shows the *salvia mirzayanii* plant and oil used in the current study.

Traditionally, a homogeneous alkaline like NaOH and KOH is used for the biodiesel production. These kinds of catalysts have a high yield and rate of reaction, but they need a great amount of water in the leaching stage leads to a great volume production of wastewater [15]. Also, the water within the oil will cause saponify and hydrolysis of side reactions, and so, the separation process will be more difficult, and consequently, the final costs increase [7].

Solid catalysts are an appropriate choice to replace the homogenous catalysts. These catalysts will not be disolved in the alcohol, so they can be easily separated with less corrosion. The biodiesel production has been recently increased using solid catalysts.

Phosphomolybdic acid (HPA) is an inorganic compound with keggin structure [16] and its chemical formula is $H_3PMo_{12}O_{40}.12H_2O$. This acid is a type of Brønsted acid that has higher acidity than sulfuric acid [17]. However, the phosphomolybdic acid is expensive with a low surface area (less than 10 m^2/g^{-1}) that easily dissolves in the polar solvents. It is hard to recover it when used as a homogenous catalyst. Therefore, the researchers dispersed HPA on the various solid supports to solve these problems [18, 19]. Gua et al. [20] synthesized a metal-organic framework (MOFs) as support for phosphomolybdic acid in the esterification reaction with a high yield close to 100% . Han et al. [21] produced biodiesel polyoxometalate based sulfonated ionic liquid. They investigated the influences of ethanol to oil molar ratio, amount of ionic liquid, and time. They achieved a maximum yield of 91.8% for the biodiesel production. It can be concluded that in these catalysts there is weak interaction between HPA and support that affects their applications in industrial processes [18].

Clinoptilolite is a natural zeolite with general chemical formula of $Na_6[(AlO_2)_6(SiO_2)_{30}].24H_2O$. It is inexpensive and available in large amount in comparison with the synthetic chemicals [22]. In addition, its inorganic framework holds them from photo-decay. Also their networks have a lot of pore and linked to the cavities and channels of nanometer sizes [23]. It has been used in many industries as adsorbent, catalyst, medicine due to aforementioned benefits. However, there are some limitations for using it in a number of industries due to the impurities in its structure [24]. Also, it is used in the trans-esterification reaction as catalyst for the biodiesel production, but, its

separation from biodiesel product is too difficult and expensive [25]. To solve this problem nano-scale magnetic catalyst can be used. Magnetic nano-particles are used as heterogeneous catalysts and have several advantages including high specific surface area, high active sites [26], high stability, physical behavior, particle size , easy operational method and high dispersion with reactants during trans-esterification reaction [27]. Magnetic catalyst can be easily separated from the reaction mixture by external magnet and reused several times. Magnetite (Fe_3O_4) is one of the magnetic nano-particles and has the strongest magnetic properties compared to other transition metal oxide [25]. Tian Li et al [28] synthesis $CaO/mSiO_2/Fe_3O_4$ as new type of heterogeneous alkali catalyst for the biodiesel production. This catalyst has high stability and activity. They could recovery of the catalyst six times without significant decrease in the biodiesel yield. Ambat et al [29] discussed properties of potassium impregnated Fe_3O_4-CeO catalyst for the biodiesel production from rapeseed oil. Rezayan and Taghizadeh [25] described the impregnation of KOH on ZSM-5-Fe_3O_4 for the biodiesel production by trans-esterification of canola oil.

Reflux method is usually used for the production of biodiesel through esterification and transesterification reaction. In this method, the system temperature should be higher than 65°C (boiling point of methanol) in order to occurring the reaction. External energy is required for the heating of system. Electrolysis method is another way for the production of biodiesel. In electrolysis method, electrical voltage generates heats which it is ample to take place reaction to produced biodiesel. Therefore, no need to use external heat from the heater or etc. So, energy saving is one of the advantages of electrolysis method. Furthermore, it should be also noted that in conventional methods, the presence of excessive amount of water causes a saponification reaction and reduction of biodiesel yield. Also, the further energy and costs are required for neutralization and purification. However, in the electrolysis method, not only the process requires the presence of water to produce biodiesel, but also the water presence enhances the yield and improve the performance of system through H^+ and OH^- ions production on the electrode surface. In addition, in conventional methods, up to 7 times washing using water is required to neutralize the biodiesel product until it reaches pH = 7, but, neutralization can be achieved by one time washing in the electrolysis method. As a result, it can be concluded that the electrolysis method saves water consumption and reduces wastewater production [30].

Putra el al [31] reported the high content of fatty acid esters (FFA) in feedstock oil doesn't cause side reaction like saponification reaction and loss of the catalyst. In the biodiesel purification steps, a little amount of water consumed, so less wastewater is produced. Therefore, the electrolysis method is environmentally friendly and is a method that saves energy. Production of biodiesel via electrolysis method was firstly reported by Guan and Kusakabe [32], they synthesized biodiesel fuel from waste cooking oil (WCO) and corn oil in the presence of NaCl catalyst with fatty acid methyl ester (FAME) and obtained yield of 97%>. Helmi et al [33] synthesized biodiesel from WCO through electrolysis method with graphite electrodes in presence of phosphomolybdic acid/graphene oxide as solid acid catalyst. They achieved the highest biodiesel yield of 90.39%.

In this research, the phosphomolybdic acid /clinoptilolite-Fe_3O_4 catalyst was synthesized and its performance was investigated through using in the production of biodiesel from *salvia mirzayanii* oil as a new non-edible source. The characterization of the catalyst was investigated by FESEM, EDX, TEM, FTIR and VSM analyses. The biodiesel production parameters were optimized by the Taguchi method. The effects of effective parameters like catalyst weight, alcohol to oil molar ratio, temperature and reaction time were tested on the biodiesel yield via analysis of variance [34] during the esterification reaction. The GC-MS, FTIR and H-NMR analysis were used to identify properties of *salvia mirzayanii* oil and biodiesel. Finally, the physical properties of biodiesel include density, viscosity, cloud, pour, and flash points were measured based on the ASTM standard.

2. Experimental

2.1. Materials

The natural clinoptilolite powder (mesh 45 μm), sodium hydroxide (99%), iron (ii) chloride (97%), iron (iii) chloride (99%), sodium sulfate (99%), methanol (99%), hydrochloric acid (37%), acetone (95%) were purchased from Merck Company, Germany. The BATE PC21 furnace, Lab Tech oven, and RLABINCOM-81 stirrer were used in the experiments of this study. The Salvia mirzayanii seed purchased from Semnan, Iran.

2.2. Oil extraction

Firstly, *salvia mirzayanii* roots and flowers were dried for a week, then crushed with mill and a certain amount of *salvia mirzayani* powder and desired volume of methanol [14] as the solvent (1:4 w/v%) were put into a round bottom flask with a volume of 250 mL, then Soxhlet apparatus which was equipped with a condenser was used for the extraction. Among various methods for the oil extraction including shaker, filtration, soxhlet apparatus and separating funnel, the soxhlet apparatus is considered superior approach for the producing crude oil from the *salvia mirzayanii* plant. It is because the method is continuous and full recovery of solvent can be obtained using the method [35]. The setup was heated by the heat mantle at a constant temperature of 60 °C until discoloration of methanol for 6 h. The vacuum distillation method using a rotary evaporator was used for solvent recovery. The residual moisture was eliminated with mixing of extracted oil with sodium sulfate (Na_2SO_4) [36]. At the end, the oil was filtered to calculate the yield of extracted oil by the following equation (1). The yield of oil extraction was 30 w/w%.

$$\text{Oil Yield} = \frac{\text{Weight of produced oil}}{\text{Weight of used sample}} \quad (1)$$

2.3. Clinoptilolite-Fe_3O_4 synthesis

Magnetic particle of clinoptilolite-Fe_3O_4 were synthesized according to the method reported by Rezayan and Taghizadeh [25] with some modifications. As can be seen in Fig. S2, $FeCl_3$ and $FeCl_2$ (2:1 molar ratio) was added to 200 mL distillate water and mechanically stirred at 70 °C. When the mixture temperature was reached at 70 °C, the NaOH solution (5 M) was added to the reaction mixture drop by drop and stirred for 30 minutes. In this stage, clinoptilolite was added to the reaction mixture and stirred for 1 h to render clinoptilolite-Fe_3O_4 (3:1 wt.% ratio). At end of the reaction, the black magnetic substance was appeared that indicates the clinoptilolite-Fe_3O_4 was formed. The reaction was performed under nitrogen gas atmosphere. A magnet was used to wash clinoptilolite-Fe_3O_4 magnetic particles. In this way, the magnet causes the magnetic particle to be placed at end of the container and easily separated from water. The clinoptilolite-Fe_3O_4

was washed using distillate water several times until the pH reached 7. The products were dried at 100°C in oven overnight and calcined in furnace at 550 °C for 6 h.

2.4. Catalyst preparation

The immobilization of phosphomolybdic acid on the clinoptilolite-Fe_3O_4 magnetic support was carried out based on the report by Avramidou et al. [37]. A colloidal suspension of the clinoptilolite-Fe_3O_4 was sonicated as support in the solvent of water for 1 h. Then, phosphomolybdic acid was dissolved in hydrochloric acid (0.1 N) and added to the reaction mixture at the constant stirring speed of 300 rpm by applying a magnetic stirrer for 24 h at room temperature. After, a vacuum rotary evaporator was used for the solvent evaporation at conditions of 90 °C and 100 rpm, and then it was dried in a vacuum oven at 100 °C for 24 h. The dried solids were squashed in an agate mortar to get a fine powder as an HPA/clinoptilolite-Fe_3O_4 magnetic solid catalyst. Finally, the catalyst was calcined at 300 °C for 3 h. When the oxygen-containing functional groups on the clinoptilolite-Fe_3O_4 surface were polarized in an acidic medium, the suitable dispersion of HPA on clinoptilolite-Fe_3O_4 was achieved with a powerful electrostatic binding.

2.5. Characterization analyses

The synthesized HPA based on clinoptilolite-Fe_3O_4 was characterized via different analyses to check its composition and structure properties. The X-ray Powder Diffraction (XRD) analysis was performed in the range of 2θ= 5-80°, with step size 0.05 deg (XRD, PHILIPS PW1730). The Fourier Transform Infrared spectroscopy (FTIR, Thermo, Avatar) demonstrated the molecular vibration characterization of catalysts and oil between 400 and 4000 cm^{-1}. The surface morphologies of the catalyst and elemental analysis were observed by Field Scanning Electron Microscopy (FESEM, Philips XL30 ESEM) and Energy Dispersive X-ray Spectroscopy (EDS, Tescan, Miraa III), and Transmission Electron Microscope (TEM, Zeiss, EM900). In order to study magnetic properties of the catalyst, a Vibrating Sample Magnetometer analysis (VSM, Meghnatis Daghigh Kavir Co. Kashan LBKFB) was used. The GC-MS of Salvia mirzayanii oil and biodiesel were carried

out on an Agilent 5973 GC and 6890 Mass Spectrometer at 250 °C as inlet temperature and auxiliary temperatures of 280 and 180 °C for 5 min.

2.6. Electrolysis method

First, 50 g of *salvia mirzayanii* oil was poured into the 100 mL cell of the reactor, then 1.3 g distilled water and 0.5-1.5 wt% catalyst to oil weight (6:1, 9:1, and 12:1 as methanol/oil ratio) was added to the cell, severally. In this condition, the reaction mixture was two-phase, so the acetone solvent was used to make it one-phase. Finally, the magnetic stirrer was applied to mix the final mixture at a speed of 100 rpm. Two electrodes of surface graphite were embedded at two sides of the reactor with a specific distance at different temperatures of 55, 65, and ٧5 °C and then connected to a DC power supply (Fig. S3). The reactor was closed tightly to prevent the evaporation of methanol and acetone, and then the voltage of ۴۰ V was finally imposed on the solution. After half an hour, the glycerin was separated from biodiesel in the experiment. However, various times were considered for the process to complete the process [38]:

$$\text{Biodiesel Yield}=\frac{\text{Weight of produced methyl ester}}{\text{Wieght of oil in reaction}}\times 100 \quad (2)$$

2.7. Design of experiments with Taguchi method

Taguchi optimization method was first reported by Taguchi [39] that mainly investigated the effects of different individual parameters for process optimization. This method is applied to solve the industrial and engineering problems by optimizing the processes with a minimum number of experiments, a lower time reaction, and lower experimental costs [35, 39, 40]. The orthogonal array (OA) technique is charted levels of a factor through the experiment [39]. Four factors include catalyst weight, methanol/oil molar ratio, temperature, and reaction time with three levels were chosen in this research presented in Table S1. The OA was created via the program based on these factors, their levels, and using Eq. (3) as follows:

$$N=(\mathrm{L}-1)\,\mathrm{P}+1 \quad (3)$$

where *N* defined as the number of runs, *L* indicates number of levels, and the symbol of *P* indicates number of parameters.

2.8. Statistical analysis including ANOVA and signal-to-noise ratio

One of the vital benefit of the Taguchi method in comparison with the other experimental design approaches is the comparison of the effects of factors on the process. These properties can be explained by ANOVA and S/N ratio. The Signal-to-Noise ratio is considered as the ratio of the biodiesel average yield to the standard deviation [41, 42] that investigates the effects of factors on the biodiesel yield. Also, the ANOVA was utilized to estimate the impacts of statistical parameters [34, 43] and calculate the contribution of effects of each factor individualistic on the final results [44]. Equation (4) is applied to evaluate effect of each factor on the process performance:

$$\%\text{Contribution of Factor} = \frac{SS_f}{SS_T} \times 100 \tag{4}$$

where SS_f and SS_t represent the sum of the square of each variable and sum of the square of all variables. SS_f and SS_t were calculated by Equation (5) and (6) [34, 36]:

$$SS_f = \sum_{j=1}^{3} n[(S/N)_{fj} - (\text{S/ N})_T]^2 \tag{5}$$

$$SS_T = \sum_{i=1}^{9} [(S/N)_i - (S/N)_T]^2 \tag{6}$$

where *n* symbol is experiment number with level (*j)* of factor (*f)* and total number (*T)*.

There are different (S/N) ratios accessible based on the output type such as 'larger the Better' (LTB), 'Lower the Better' (LTB), and 'Nominal is the Best' (NB). Based on data properties, (LTB) was chosen to achieve maximize biodiesel yield and it was calculated using Eq. (7):

$$S/N = -10\log\left[\frac{1}{n}\sum_{i=1}^{n}\frac{1}{y_i^2}\right] \tag{7}$$

where *i*, y_i, and *n* display the number of design factors, the measured values, and the number of the experiment, respectively. All experimental runs were used to develop a statistical regression by taking into account all parameters into the regression model. This model can estimate the biodiesel yield under the constant process conditions and connect the predicted response to the actual response [42, 44].

2.9. Physicochemical properties of synthesized biodiesel

The chemical and physical properties of synthesized biodiesel were determined by standards method offered via American Society for Testing and Materials (ASTM). The fuel properties include flash point, kinematic viscosity, cetane number, and density were measured and compared with the commercial diesel. Other synthesized fuel properties such as cloud point, Cold Filter Plugging Point, and pour point were estimated based on standard methods [45]. The characterization of oil and the quality of biodiesel was examined through the H-NMR analysis that 50 µl of sample was dissolved into 600 µl of the solvent of chloroform ($CDCl_3$) with a scan rate of 32. The chloroform was handled as the internal standard.

3. Results and discussion

3.1. Oil and biodiesel characterization

GC-MS result of oil and biodiesel are illustrated in Fig. S4 and S5, respectively. The combination of the oil and biodiesel were measured and compared to the NIST database shown in Table S2 and Table S3, respectively. Based on the table data, four major free fatty acids are presented in the oil affected the stability and properties of biodiesel. Also, it can be concluded that the unsaturated fatty acid is more than 80% of the primary feedstock. The most content of the unsaturated fatty acid is established the linoleic acid with 16.28%. The unsaturated fatty acid causes oxidation of fuel due to having double bonds [46]. The *salvia mirzayanii* oil was dark red-brown in color with no smell. No water and other impurities were presented in the oil, and the acid value was 2.24 mg KOH/g oil. The viscosity and density were 15 mm^2/S and 0.932 g/cm^3, respectively. The iodine value, saponification value and cetane number of *salvia mirzayanii* oil were 105.43 (g of I_2/100 g of oil), 193 (mg of KOH/g of oil), and 68 respectively. So, the *salvia mirzayanii* oil was an appropriate feedstock to carry out trans-esterification reaction with the HPA/clinoptilolite-Fe_3O_4 catalyst for the biodiesel production.

The GC-MS analysis of biodiesel produced under optimum condition was shown in Fig S5 and Table. S3. Based on the results, four major peaks were presented in GC-MS analysis and each peak belongs to an unsaturated or saturated fatty acid methyl ester in the biodiesel. Results of GC-MS analysis confirm that the biodiesel contains 8,11-octadecadienoic acid methyl ester (45.39%), oleic acid methyl ester (36.73%) and methyl palmitate (12.93%). These fatty acid methyl esters contain carbon double band that affect the oxidation stability and degree of saturation. Therefore, due to occurrence of high amount of 8,11-octadecadienoic acid methyl ester and oleic acid methyl ester in Salvia mirzayanii biodiesel, it has little oxidation stability and high degree of saturation.

3.2. Catalyst characterization

3.2.1. Field emission scanning electron microscopy and Energy Dispersive X-ray analyses

The surface morphology and elemental compounds of clinoptilolite as raw support and HPA/clinoptilolite-Fe_3O_4 as the catalyst were investigated using FESEM and energy dispersive X-ray (EDX) depicted in Fig .1 (a). The spherical morphology on the unruly surface [47] and leaf-like structure of clinoptilolite with nano diameter [48] indicated in Fig. 1 (a). Table S4 presents the EDX analysis that indicates the clinoptilolite has aluminum, iron, silicon, and potassium and oxygen elements.

FESEM image of clinoptilolite-Fe_3O_4 (Fig. 1 (b)) displays that this catalyst support has separated irregular aggregates with spherical-like shape (gray parts). These increase the specific surface area of clinoptilolite-Fe_3O_4 [49]. Base on the Table S4 and the EDX results, the weight percentage of iron element has been increased in clinoptilolite-Fe_3O_4. Fig. 1 (c) shows the HPA particles found on the surface of clinoptilolite-Fe_3O_4 sheets and its significantly rough surface. The EDX analysis revealed the presence of molybdenum, phosphor, aluminum, iron, silicon, and potassium and oxygen that affirms the successful incorporation of HPA on the clinoptilolite-Fe_3O_4 (Table S4).

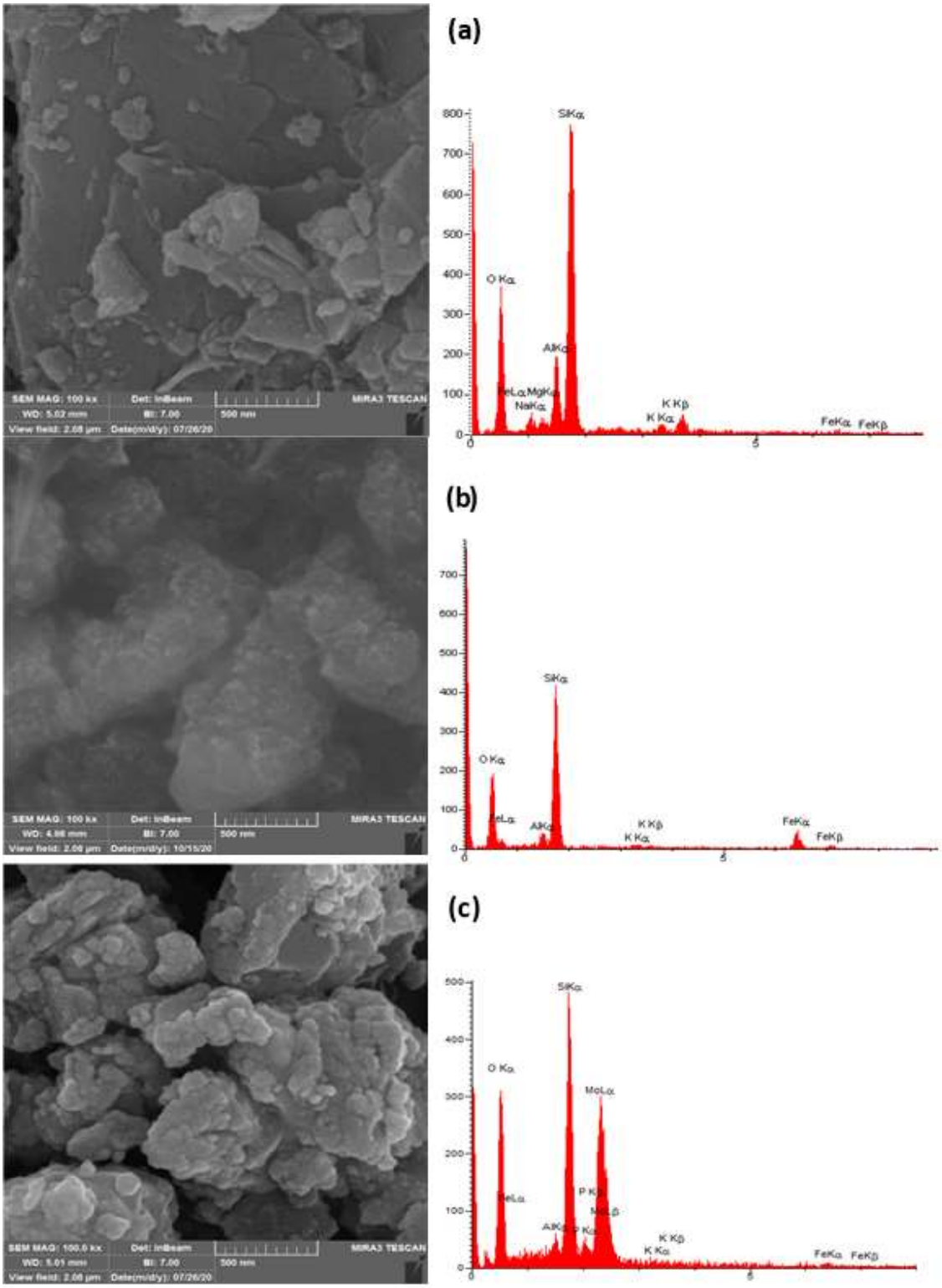

Fig. 1. FESEM and EDX analyses for (a) clinoptilolite, (b) clinoptilolite-Fe_3O_4 and (c) HPA/clinoptilolite-Fe_3O_4 catalyst

3.2.2. Transmission electron microscopy analysis

Morphology surface of raw clinoptilolite and HPA/clinoptilolite-Fe_3O_4 as magnetic catalyst with better quality shows in TEM images (Fig .2). Fig .2a indicates spherical-like structure of clinoptilolite [47]. TEM image of HPA/clinoptilolite-Fe_3O_4 illustrates (Fig .2b) HPA clusters as dark points on clinoptilolite-Fe_3O_4 surface that shows HPA and Fe_3O_4 successful immobilization on clinoptilolite surface. Also, immobilization of HPA doesn't effect on clinoptilolite structure.

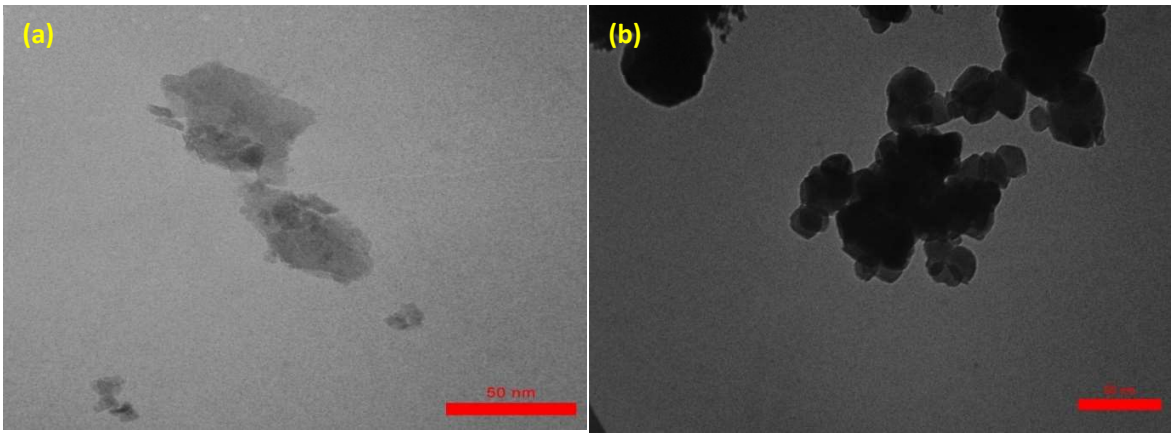

Fig. 2. TEM of (a) clinoptilolite and (b) HPA/clinoptilolite-Fe_3O_4 catalyst

3.2.3. FTIR analysis

FTIR spectra of clinoptilolite, HPA, clinoptilolite-Fe_3O_4 and HPA/clinoptilolite-Fe_3O_4 catalyst was shown in Fig. S6. The FTIR of clinoptilolite indicated stretching vibration at 3442 cm^{-1} that related to the hydroxyl groups (-OH), the binding vibration of hydroxyl groups (-OH) of clinoptilolite surface at 1636 cm^{-1}. The strong band at 1067 cm^{-1} and 795 cm^{-1} was observed which are generic asymmetric vibration of Si-O-Si and stretching vibration of Si-O groups, respectively [48], these peaks confirming silicon and aluminum presence on the surface of clinoptilolite. The peak at 607 cm^{-1} belongs to the Si-O-Si and Si-O-Al bending vibration [24]. To understand the interaction between clinoptilolite and Fe_3O_4, the FTIR spectroscopy was investigated. The main peaks of raw clinoptilolite observed in FTIR spectra of clinoptilolite-Fe_3O_4. However, the transmittance percentage (%T) of many peaks was changed but their wavenumber was unchanged. The new peaks appeared at 400-700 cm^{-1} were assigned to bond of Fe-O of Fe_3O_4. The Fe-O strong

absorption bands have peaks at 468 cm^{-1} and 521 cm^{-1}. Overall the peaks less than 700 cm^{-1} related to Fe-O bond [49]. These peaks confirmed coating of Fe_3O_4 particles on the surface of clinoptilolite. Phosphomolybdic acid of keggin structure has peaks at 1064 cm^{-1}, 963 cm^{-1}, 870 cm^{-1} and 789 cm^{-1} which related to stretching frequency of P-O_a in the PO_4, stretching bands of the terminal Mo=O_d in the exterior MoO_6, octahedral corner sharing Mo-O_b-Mo and octahedral edge sharing Mo-O_c-Mo [18, 50, 51]. The presence of main peaks of HPA and clinoptilolite-Fe_3O_4 in HPA/clinoptilolite-Fe_3O_4 FTIR spectrum indicates strong electrostatic interaction between HPA clusters and the clinoptilolite-Fe_3O_4. It can be concluded due to existence of the large number of the oxygen functional groups on the clinoptilolite surface [52].

3.2.4. X-ray diffraction spectroscopy

XRD spectra of raw clinoptilolite and the HPA/clinoptilolite-Fe_3O_4 catalyst are illustrated in Fig. S7 The XRD spectra of clinoptilolite has main peaks occur at 2θ= 11.19°, 13.01°, 17.51°, 19.01°, 21.74°, 22.46°, 26.18°, 28.23°, 37.21° from the (324.87), (206.88), (428.57), (223.86), (870.08), (2209.95), (930.32), (716.72) and (409.93). The peaks characterization showed that raw clinoptilolite has crystalline structure and in accordance with XRD pattern of JCDBS 38-0237 [53]. Its main phase had a generic clinoptilolite structure. After coating of Fe_3O_4 nano particles on the surface of raw clinoptilolite, the new peaks were observed at 2θ= 36.33°, 54.39°, 62.83° areas associated to the (351.23), (142.99) and (174.99). These peaks confirmed that the face-centered cubic Fe_3O_4 nanoparticles. After immobilization of HPA on clinoptilolite-Fe_3O_4 as magnetic support the new peaks appeared at 2θ=26.49°, 27.95° and 41.77° areas which related to the (1053.09), (980.42) and (286.35) [23]. The *Debye–Sherrer's* formula was used for the calculation of average particle size of HPA/clinoptilolite-Fe_3O_4 catalyst according to the XRD data.

$$D = 0.98\lambda/\alpha \cos\theta \quad (8)$$

where D and λ are average particle size (nm) and the wave length of X-ray, respectively. The α and θ are width line at half maximum of the diffraction peak and Bragg angle in degree, respectively. Through computation, the average particle size of the magnetic catalyst was achieved 45 nm.

3.2.5. Vibrating sample magnetometer analysis

The magnetic properties of HPA/clinoptilolite-Fe_3O_4 catalyst was investigated by VSM analysis. Its hysteresis loops are shown in Fig. S8 The VSM results displayed that the HPA/clinoptilolite-Fe_3O_4 has magnetic behavior at room temperature [54]. The value of magnetic saturation (MS) of 10.57 emu/g was obtained for the sample. Firouzjaee and Taghizadeh [55] reported the MS of the magnetic solid catalyst is enough for the magnetic separation by external magnetic.

3.3. Statistical analysis

Taguchi L9 experiment design was applied for the optimization of biodiesel production from *salvia mirzayanii* oil in the presence of HPA/clinoptilolite-Fe_3O_4 as the solid magnetic catalyst. The experimental runs were tested under various conditions proposed by the experimental matrix shown in Table 1. The variation of biodiesel yield was performed by the statistical analysis to create a valid mathematical equation, optimize the process, and evaluate the individual effects of each factor via ANOVA analysis [40, 44].

Table 1. Experimental design matrix and the result of response developed via Taguchi method.

Run no.	Catalyst Wight (wt%)	Methanol/oil molar ratio	Time (h)	Temperature (°C)	Biodiesel yield
1	0.5	6:01	8	55	74.42
2	0.5	9:01	16	65	76.21
3	0.5	12:01	24	75	77.16
4	1	6:01	16	75	74.89
5	1	9:01	24	55	71.45
6	1	12:01	8	65	75.70
7	1.5	6:01	24	65	68.60
8	1.5	9:01	8	75	75.12
9	1.5	12:01	16	55	71.02

Important tests like Fisher's statistical test (F-value) and probability value (p-value) can be achieved by the ANOVA analysis. High F-value shows high consistency of the data with the linear model compared to the mean model [44]. For each factor, the high values for the summation of squares (SS) and F-value indicate that the factor has particular importance in obtaining the desired response. The p-value less than 0.05 depicts a significant effect of the selected factor. Based on ANOVA analysis, it can be deduced that four selected factors have significant impacts

on the biodiesel yield as the response. Among these factors, the catalyst weight has the highest contribution to the biodiesel yield, while temperature has the least one [40, 44]. Table 2 shows the results of the ANOVA analysis for model and process factors.

Table 2. ANOVA results for model and process factors.

Sources	DF	Adj SS	Adj MS	F-value	P-value probability>F	
Regression	4	62.737	15.6842	38.28	0.002	Significant
A-catalyst weight	1	28.253	28.2534	68.95	0.001	Significant
B-Methanol to oil molar ratio	1	5.940	5.9401	14.50	0.019	Significant
C-Time	1	10.827	10.8237	26.42	0.007	Significant
D-Temperature	1	17.716	17.7160	43.24	0.003	Significant
Error	4	1.639	0.4097			
Total	8	64.376				

The correlation coefficient is estimated for the whole process illustrated in Table 3. Estimated correlation confidence (R^2) indicates that the model is in good agreement with the experimental data. The actual and predicted values are reasonably closed by an R^2 value of 0.9745. The predicted R^2 is 0.8541, while the value of adjustment R^2 is 0.949. Difference between pre-R^2 and adj-R^2 is less than 0.2, so it can be concluded that the model used has an exact fit to our experimental data [44]. Total mean of the biodiesel yield was obtained 79.84%. Also, total signal to noise value was 38.0745. It means that model has the capability to predict the biodiesel yield as response and optimize the biodiesel production process. In present study, PRESS value (predicted residual sum of square) for the proposed model was evaluated for any data point is 81.48 that shows each point was coordinated good in the design. The coefficient variance (CV%) lower value shows the model can be predicted with high accurate. In this research CV% is 3.84 [42, 45]. The coefficient of variance is given in Table S5. According to the obtained result, the reaction time has lowest influence on the biodiesel yield with a contributing factor of 9.23%, and catalyst weight contribution is dominant with the highest contribution of 43.9% [40].

Table 3. Statistical factors estimated by the ANOVA analysis.

Parameter	Value	Parameter	Value
Predicted R^2	0.8541	R^2	0.9745
Coefficient of variance (%)	73.844	Adjusted R^2	0.9491
S/N ratio	38.0745	Mean	79.8467
C.V%	3.84	BIC	45.41
PRESS	81.48	AICc	112

3.3.1. Regression model equation development and validation

Regression model for the biodiesel yield based on the experimental data was given in Eq. (8). The coded equation is recognized the effect of each factors by comparing the contribution of each factor and can predict optimum condition for the factors within the selected levels [56]. The model includes four factors of catalyst weight, methanol to oil molar ratio, reaction time, and temperature with the lower and upper levels of -1 and +1, respectively.

$$\begin{aligned} Biodiesel\ yield &= 73.84 + 2.086A[1] + 0.1689A[2] - 2.254A[3] - 1.208B[1] + 0.4256B[2] \\ &+ 0.7822B[3] + 1.246C[1] + 0.1956C[2] - 1.441C[3] - 1.548D[1] - 0.3411D[2] + 1.889D[3] \end{aligned} \quad (9)$$

where A[57], A[57], and A[3] are catalyst weight at, B[57], B[57], and B[3] are methanol to oil molar ratio, C[57], C[57], and C[3] are time, and D[57], D[57], and D[3] are the temperature at 1st, 2nd and 3rd levels, respectively, presented in Table 1. The experimental and predicted values are plotted in Fig. 3. From this figure, it can be concluded that the actual and predicted values are almost in a straight line, and the model was accurately calculated the response of biodiesel yield [42, 56].

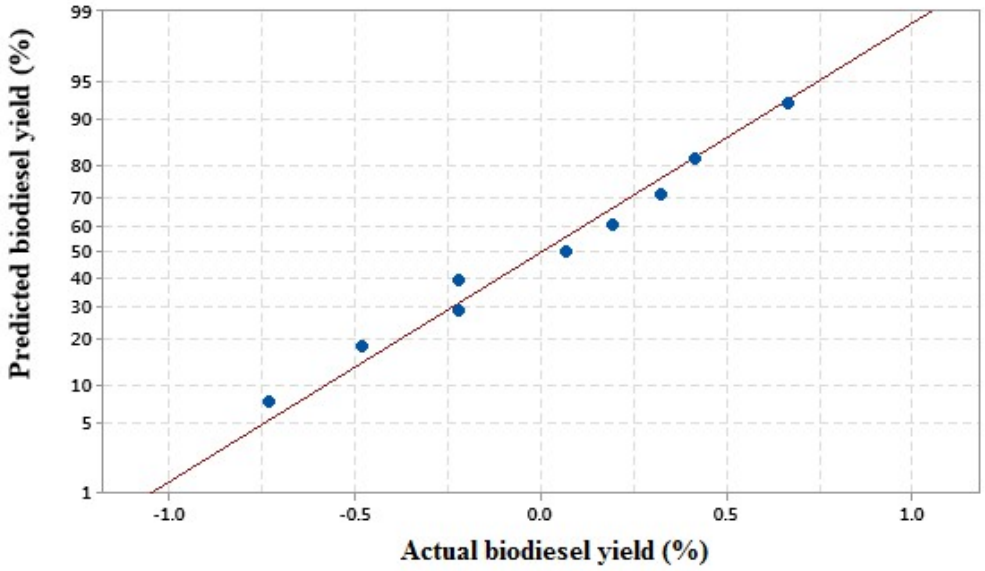

Fig. 3. Predicted and actual biodiesel yields.

3.4. Optimization by Taguchi method

In this study, the effects of catalyst weight, methanol to oil molar ratio, reaction time, and temperature as the influential factors on the biodiesel yield are investigated. The experimental runs were carried out based on Taguchi L9 design to obtain the optimal conditions to reach the highest yield. Also, the individual effects of each factor on the experimental response of each run are examined under different conditions [42, 56].

3.4.1. Influence of catalyst weight

Catalyst weight impact on the biodiesel production process is investigated by variation of the catalyst loading from 0.5 to 1.5 wt.% for the *salvia mirzayanii* oil. As can be observed in Fig. 4 (a), the biodiesel yield decreases by enhancing the catalyst weight from 0.5 to 1.5 wt.% due to the active site enhancement on the surface of the HPA/clinoptilolite-Fe_3O_4 catalyst. In this condition, the side reaction is performed on the unused active sites of the catalyst leads to increment in the viscosity of reaction mixture. High amounts of the catalyst harm biodiesel production that makes the reaction reversible. The biodiesel product is also absorbed by the excess catalyst, and thereby the final yield reduces [2, 58].

3.4.2. Influence of methanol to oil molar ratio

The methanol to oil molar ratio has considerable influence on the biodiesel production process. Fig. 4 (b) indicates that the biodiesel yield enhances by changing the methanol to oil ratio from 6 to 12. An increase in the amount of methanol improves the trans-esterification reaction towards biodiesel due to its reversible reaction [59]. However, an increment in the methanol reduces the biodiesel yield. The excess amount of methanol decreases the weights of the reactant and catalyst, so the reaction is delayed. Besides, the solvent recovery is hard at high methanol to oil ratios, and the biodiesel product forms an emulsion during the washing step [60].

3.4.3. Influence of reaction time

The reaction time is an inevitable factor to optimize the biodiesel production reaction. As can be observed in Fig. 4 (C) for the HPA/clinoptilolite-Fe_3O_4 catalyst, the biodiesel yield enhances by the enhancement of the reaction time from 8 to 16 h because of a strong interaction between the catalyst and reaction mixture [61]. But the conversation of biodiesel decreases slightly by increasing the time to 24 h due to constitution water emulsion as the product of the ahead reaction [56].

3.4.4. Influence of reaction temperature

The reaction temperature is important in the production of biodiesel. As given in Fig. 4 (d), the reaction rate and biodiesel yield rise by the enhancement of the reaction temperature from 55 to 75 °C. It is because the oil viscosity is reduced and the oil to biodiesel conversion is enhanced at high temperatures [25]. Also, the contact between methanol and the reaction mixture is reduced during the methanol evaporation at high temperatures. Therefore, a temperature of 75 °C near the boiling point of the methanol was chosen as the optimal temperature to prevent the evaporation and loss of methanol [62].

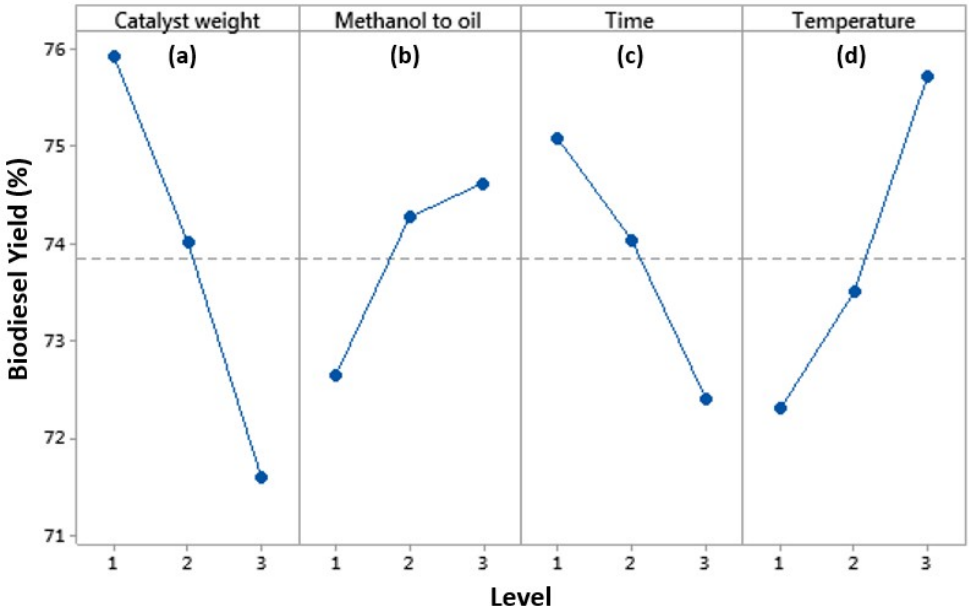

Fig. 4. The effect of (a) catalyst weight (b) methanol to oil molar ratio (c) reaction time and (d) temperature on the biodiesel yield.

3.5. Fourier transform infrared spectroscopy (FTIR) analysis of *salvia mirzayanii* oil and biodiesel

After finishing the trans-esterification process and the separating and purification steps, the FTIR spectrum was performed on the *salvia mirzayanii* oil and sample to ensure that the biodiesel is produced. Based on Fig. S9, the FTIR spectrum of oil indicates the peaks at 1166.43-1377.59 cm^{-1} region related to binding vibration of the overlapping three groups C-O ester. The peaks appears at 1655.84-17٥٤,٦ cm^{-1} region associated to three carbonyl functional groups (C=O) of triglyceride oil. The characterization peaks at 1377.59 cm^{-1} and 1464.45 cm^{-1} relate to the bending vibration of the alkyl C-H groups linked to strong oxygen adsorption [63]. The main difference between FTIR spectrum of oil and biodiesel are these peaks because the FTIR of biodiesel doesn't have them [64]. Bending vibration of C-H Alkyl groups have peaks at 2856.25 cm^{-1}. The peak at 3008.38 cm^{-1} shows –OH group of water [65]

Only difference between the oil and biodiesel is in the 1000-1500 cm^{-1} range that indicates the glycerol exits. The most important index peaks in the biodiesel FTIR spectrum is related to the bending and kinetic vibrating of O-CH_3 functional group at 1241.75 and 1170.08 cm^{-1}

wavenumbers, respectively. The alkyl C-H bending vibration causes two peaks that appeared at 1362.74 and 1460.75 cm^{-1} regions.

The carbonyl-ester and alkyl C-H bending vibrations have peaks at wavenumbers of 1743.27 and 2854.12 cm^{-1}, respectively. One of the most important contaminants of fuel is water. The presence of water causes corrosion in the contaminant tank, storage, and transportation instruments [66]. It is also frozen at low temperatures and districted the fuel flow [67]. So, the biodiesel might have impurities such as monoglyceride, diglyceride, water, and free fatty acids that have the OH functional group seen in the 3000-3200 cm^{-1} range. If there were not any peaks in this area or appeared with a short peak, this will show the desired purity of the produced biodiesel [61]. Based on the reported of Huang et al [68] FTIR spectrum of biodiesel confirms that the trans-esterification was successful and biodiesel (methyl ester) fuel with similar physicochemical properties of commercial diesel was produced. Tariq et al [69] showed that the FTIR spectrum of *salvia mirzayanii* oil and biodiesel are similar together but the main difference could be seen in the shifting peaks at 1754.61, 1377.59, 1166.43 and 916.98 cm^{-1} to 1743.27, 1360.55, 1170.08 and 847.29 cm^{-1} in the produced biodiesel, respectively. Disappearing of the peaks at 1464.45, 1098.88 and 960.12 cm^{-1} as well as appearing of peaks at 1460.72 and 1170.08 cm^{-1} in the FTIR spectrum means that the *salvia mirzayanii* oil was conversated into biodiesel.

3.6. Analysis of biodiesel by H-NMR

The H-NMR spectra of salvia mirzayanii oil (Fig. S10) shows the peaks at 0.90 ppm and 1.126-1.31 ppm attributed to the methyl hydrogens of the linolenic acyl groups (-CH_3) and the acyl groups (-$(CH_2)_n$-), respectively. The peaks at 1.62 ppm and 2-2.34 ppm refer to acyl groups (-OCO-CH_2-CH2) of oleic acid and acyl group (-OCO-CH_2-), respectively. It seems that the peaks at 4.12-4.35 ppm exclusively related to glyceryl group (-CH_2OCOR). The peaks at 5.35-5.36 associated to the acyl groups (-CH=CH-) [70].

H-NMR study was performed to confirm that the biodiesel produced from *salvia mirzayanii* in presence of HPA/clinoptilolite-Fe_3O_4 catalyst (Fig. S11). The terminal alkyl methyl protons present in biodiesel have peaks at a domain of 0.80-0.83 ppm. The sharp peaks at 1.20 and 1.25 ppm due to presence of carbon chain methylene protons [33]. The double bond carbon related to the α-

CH_2 is at the range of 1.94-2.00 ppm. The β-methylene groups in the methyl esters have peaks at 2.23 ppm. The triplet peak at 2.26 ppm was corresponding to the α-methylene protons (-C=C-CH_2-C=C-). The singlet peak display at 3.59 ppm particularly dependent with the methyl esters (biodiesel). Additionally, the olefinic hydrogens (-CH=CH-) have peaks with low intensity at 5.27-5.29 ppm [71].

3.7. Physical and chemical properties

The synthesized biodiesel physicochemical properties at optimum conditions were measured using the ASTM standard method presented in Table S6. The cetane number (CN) shows the ignition delay of fuel in which the higher CN value is better for the combustion effect [42]. In the present study, the cetane number is 34.77 that is higher than the CN of commercial diesel fuel, and so it is acceptable for the ASTM standard. The flash point is a parameter that identifies the lowest temperature that the fuel vaporizes and arranges a burnable mix with air [42]. The optimum flash point is 130 °C for the produced biodiesel that shows this fuel has high thermal stability [72]. Also, the cloud point is more important than the pour point because it illustrates fuel flow ability [1]. The cloud point and pour point of the optimum biodiesel were 4°C and -6°C, respectively. From the results, this biodiesel is suitable for cold areas due to its low cloud and pure points. Finally, the density and viscosity are the main parameters for injection and combustion [73], and also, the viscosity gives some information about acidic properties and fluidity of the fuel [1]. The density and viscosity were obtained 0.882 g/cm^3 and 3.08 mm^2/S, respectively. All measured properties were in good agreement with the ASTM standard, and some of them were better than the commercial diesel.

3.8. Mechanism of biodiesel production

In order to biodiesel production with high yield, one of the important steps is using an appropriate catalyst. The HPA/Clinoptilolite-Fe_3O_4 consisted of phosphomolybdic acid (HPA) as active site and Clinoptilolite-Fe_3O_4 as magnetic support. The HPA is the main key in mechanism of biodiesel production is mainly affected by the type of active site (HPA while the Clinoptilolite-Fe_3O_4 as support role is the improvement of HPA properties and its uniform distribution on the

surface of support. In the 1st step of biodiesel production, oxygen of carbonyl group is protonated with acidic catalyst (HPA). Then, in 2nd step, nucleophile (H_2O molecule) attacks to the protonated carbonyl because its oxygen has higher positive charge in comparison with neutral oxygen. Then, a balance is created between protonated tetrahedron and its non-protonated form. Then, oxygen atom of ester groups of triglyceride oil is protonated. The balance in third and fourth steps shows the rearrangement of proton group. In final step, tetrahedral of intermediate compound is collapsed and it can result in regeneration of H^+. Therefore, free fatty acid and glycerol molecules are produced. Then, the hydrolysis reaction is carried out in this pathway which leads to the production of monoglycerides and fatty acid (Fig. S12) [74].

3.9. Catalyst reusability

As mentioned in the previous sections, the reusability is an economic characteristic in the heterogeneous catalysts [4]. Therefore, the reusability of the HPA/clinoptilolite-Fe_3O_4 catalyst is investigated in this study. For this propose, the catalyst was firstly separated via magnet, and then washed with n-hexane and methanol to remove the polar and nonpolar impurities, and finally dried at the oven for 2 h at 70 °C. Based on Fig. S13, the HPA/clinoptilolite-Fe_3O_4 catalyst was used four times with the highest and lowest biodiesel yield of 80% and 71%, respectively. It can be concluded that the catalyst activity and the yield was reduced in each cycle compared to the previous cycle. The pore volume, surface area and pore size of fresh catalyst and reused catalyst were investigated by BET measurement. The BET analysis results were summarized in Table S7. According to the BET results, the surface area of fresh HPA/clinoptilolite-Fe_3O_4 was reduced from 0.96885 m^2/g to 0.32275 m^2/g after four cycles. These reductions are due to large molecules of oil, moisture, and other impurities adsorbed on the catalyst surface and it causes deactivation of its active sites. Also, it can be concluded that the presence of large molecules of oil and other impurities on the catalyst surface reduce the catalyst activity.

4. Conclusion

In this study, *salvia mirzayanii* oil was characterized and applied as a feedstock for the biodiesel production in the presence of HPA/clinoptilolite-Fe_3O_4 as the solid magnetic catalyst via electrolysis method. The catalyst was prepared by the immobilization of HPA (40%) on the clinoptilolite-Fe_3O_4 as the magnetic support. The properties of the HPA/clinoptilolite-Fe_3O_4 catalyst were evaluated by the FESEM, EDX, TEM, FTIR, XRD and VSM analyses. The effects of catalyst weight, methanol/oil ratio (molar), reaction time, and temperature on the trans-esterification were examined and optimized using the Taguchi method. The highest conversion yield of *salvia mirzayanii* oil to biodiesel was obtained at 0.5 wt.% catalyst weight, methanol to oil molar ratio of 12:1, 75 °C, and 8 h reaction time. The contribution factors were 43.9, 27.52, 16.81 and 9.23 for catalyst weight, temperature, time, and methanol to oil molar ratio, respectively, based on the statistical analysis. The high value of the correlation coefficient confirmed the accuracy and validity of the model. The physicochemical properties of synthesized biodiesel were measured by the ASTM method and compared with conventional diesel. An agreement with the ASTM standard and an improvement relative to conventional diesel were observed. As a main result, the clinoptilolite-Fe_3O_4 as the magnetic support has a high specific area and oxygenated functional groups that help to immobilize the HPA as an active site on the clinoptilolite-Fe_3O_4. Furthermore, the HPA/clinoptilolite-Fe_3O_4 catalyst was recycled four times without any significant reduction in the biodiesel production efficiency and BET analysis results of fresh and reused catalyst showed surface area of reused catalyst was decreased because of absorbent of large molecular of oil and impurities in catalyst surface.

References

[1] R.M. Ali, M.R. Elkatory, H.A. Hamad, Highly active and stable magnetically recyclable CuFe2O4 as a heterogenous catalyst for efficient conversion of waste frying oil to biodiesel, Fuel 268 (2020) 117297.

[2] M.-C. Hsiao, J.-Y. Kuo, S.-A. Hsieh, P.-H. Hsieh, S.-S. Hou, Optimized conversion of waste cooking oil to biodiesel using modified calcium oxide as catalyst via a microwave heating system, Fuel 266 (2020) 117114.

[3] K.B.Z.F. Branco, W. Balmant, E. Trevisan, D.M. Taher, A.B. Mariano, P.A. Arroyo, Phenomenological modeling of Acutodesmus obliquus microalgae in situ transesterification, Biochemical Engineering Journal 154 (2020) 107434.
[4] H. Zhang, H. Li, H. Pan, A. Wang, C. Xu, S. Yang, Magnetically recyclable basic polymeric ionic liquids for efficient transesterification of Firmiana platanifolia L.f. oil into biodiesel, Energy Conversion and Management 153 (2017) 462-472.
[5] M. Helmi, K. Tahvildari, A. Hemmati, Parametric optimization of biodiesel synthesis from Capparis spinosa oil using NaOH/NaX as nanoheterogeneous catalyst by response surface methodology, Brazilian Journal of Chemical Engineering (2020) 1-15.
[6] M. Helmi, A. Hemmati, K. Tahvildari, Biodiesel Production from Amygdalus scoparia Using KOH/Al2O3 Catalyst: Optimization by Response Surface Methodology, Iranian (Iranica) Journal of Energy & Environment 12 (2021) 34-44.
[7] J.F.O. Granjo, B.P.M. Duarte, N.M.C. Oliveira, Integrated production of biodiesel in a soybean biorefinery: Modeling, simulation and economical assessment, Energy 129 (2017) 273-291.
[8] J.-Z. Liu, Q. Cui, Y.-F. Kang, Y. Meng, M.-Z. Gao, T. Efferth, Y.-J. Fu, Euonymus maackii Rupr. Seed oil as a new potential non-edible feedstock for biodiesel, Renewable Energy 133 (2019) 261-267.
[9] P.R. Pandit, M.H. Fulekar, Biodiesel production from microalgal biomass using CaO catalyst synthesized from natural waste material, Renewable Energy 136 (2019) 837-845.
[10] S.S. Hoseini, G. Najafi, A. Sadeghi, Chemical characterization of oil and biodiesel from Common Purslane (Portulaca) seed as novel weed plant feedstock, Industrial Crops and Products 140 (2019) 111582.
[11] A. Ziaei, Z. Amirghofran, J. Zapp, M. Ramezani, Immunoinhibitory Effect of Teuclatriol a Guaiane Sesquiterpene from Salvia mirzayanii, Iranian Journal of Immunology 8 (2011) 226-235.
[12] M. Mohammadhosseini, Chemical Composition of the Volatile Fractions from Flowers, Leaves and Stems of Salvia mirzayanii by HS-SPME-GC-MS, Journal of Essential Oil Bearing Plants 18 (2015) 464-476.

[13] M.M. Zarshenas, L. Krenn, Phytochemical and Pharmacological Aspects of Salvia mirzayanii Rech. f. & Esfand, Journal of Evidence-Based Complementary & Alternative Medicine 20 (2014) 65-72.

[14] M. Khajeh, A. Ghanbari, N. Panjehkeh, M. Kaykhaii, M. Mirmoghaddam, H. Hashemi, The Essential Oils Composition of Salvia mirzayanii, Journal of Essential Oil Bearing Plants 13 (2010) 432-439.

[15] N.A. Ihoeghian, M.A. Usman, Exergetic evaluation of biodiesel production from rice bran oil using heterogeneous catalyst, Journal of King Saud University - Engineering Sciences 32 (2020) 101-107.

[16] M. Chrzanowski, M. Kliczkowski, P. Bieganski, E. Placzek-Popko, J. Misiewicz, A. Podhorodecki, Enhanced transparency of ultrathin Ag films through wetting layer of phosphomolybdic acid, Thin Solid Films 694 (2020) 137734.

[17] I. Pires de Oliveira, A.R.L. Caires, Molecular arrangement in diesel/biodiesel blends: A Molecular Dynamics simulation analysis, Renewable Energy 140 (2019) 203-211.

[18] A.K. Dizaji, B. Mokhtarani, H.R. Mortaheb, Deep and fast oxidative desulfurization of fuels using graphene oxide-based phosphotungstic acid catalysts, Fuel 236 (2019) 717-729.

[19] S. Sampurnam, T. Dhanasekaran, S. Muthamizh, A. Padmanaban, S. Munusamy, D. Latha, V. Narayanan, Synthesis, Characterization,and Photocatalytic activity of Silver nanoparticledoped Phosphomolybdic acid supportedZirconia, Materials Today: Proceedings 14 (2019) 558-562.

[20] T. Guo, M. Qiu, X. Qi, Selective conversion of biomass-derived levulinic acid to ethyl levulinate catalyzed by metal organic framework (MOF)-supported polyoxometalates, Applied Catalysis A: General 572 (2019) 168-175.

[21] X.-X. Han, Y.-F. He, C.-T. Hung, L.-L. Liu, S.-J. Huang, S.-B. Liu, Efficient and reusable polyoxometalate-based sulfonated ionic liquid catalysts for palmitic acid esterification to biodiesel, Chemical Engineering Science 104 (2013) 64-72.

[22] M. Bahrami, A. Nezamzadeh-Ejhieh, Effect of the supported ZnO on clinoptilolite nano-particles in the photodecolorization of semi-real sample bromothymol blue aqueous solution, Materials Science in Semiconductor Processing 30 (2015) 275-284.

[23] M. Bagherzadeh, H. Hosseini, Nanocluster polyoxomolybdate supported on natural zeolite: a green and recyclable catalyst for epoxidation of alkenes, Journal of Coordination Chemistry 70 (2017) 2212-2223.
[24] T. Amiri-Yazani, R. Zare-Dorabei, M. Rabbani, A. Mollahosseini, Highly efficient ultrasonic-assisted pre-concentration and simultaneous determination of trace amounts of Pb (II) and Cd (II) ions using modified magnetic natural clinoptilolite zeolite: Response surface methodology, Microchemical Journal 146 (2019) 498-508.
[25] A. Rezayan, M. Taghizadeh, Synthesis of magnetic mesoporous nanocrystalline KOH/ZSM-5-Fe3O4 for biodiesel production: Process optimization and kinetics study, Process Safety and Environmental Protection 117 (2018) 711-721.
[26] V.M. Fedorova, S.A. Kobets, L.N. Puzyrnaya, G.N. Pshinko, A.A. Kosorukov, Clinoptilolite/Fe3O4: a magnetic sorbent for removing 90Sr from aqueous media, Radiochemistry 59 (2017) 495-499.
[27] S. Tang, L. Wang, Y. Zhang, S. Li, S. Tian, B. Wang, Study on preparation of Ca/Al/Fe3O4 magnetic composite solid catalyst and its application in biodiesel transesterification, Fuel Processing Technology 95 (2012) 84-89.
[28] T.-T. Li, Y. Liu, S.-C. Qi, X.-Q. Liu, L. Huang, L.-B. Sun, Calcium oxide-modified mesoporous silica loaded onto ferriferrous oxide core: Magnetically responsive mesoporous solid strong base, Journal of colloid and interface science 526 (2018) 366-373.
[29] I. Ambat, V. Srivastava, E. Haapaniemi, M. Sillanpää, Nano-magnetic potassium impregnated ceria as catalyst for the biodiesel production, Renewable Energy 139 (2019) 1428-1436.
[30] M. Sarno, E. Ponticorvo, D. Scarpa, Novel Pt-Ni/NiO/Ni2O3 based electrodes for electrocatalytic biodiesel production from waste palm oil, Materials Today: Proceedings 20 (2020) 69-73.
[31] R.S. Putra, K. Pratama, Y. Antono, M. Idris, J. Rua, H. Ramadhani, Enhanced electrocatalytic biodiesel production with chitosan gel (hydrogel and xerogel), Procedia engineering 148 (2016) 609-614.
[32] G. Guan, K. Kusakabe, Synthesis of biodiesel fuel using an electrolysis method, Chemical Engineering Journal 153 (2009) 159-163.

[33] M. Helmi, K. Tahvildari, A. Hemmati, A. Safekordi, Phosphomolybdic acid/graphene oxide as novel green catalyst using for biodiesel production from waste cooking oil via electrolysis method: Optimization using with response surface methodology (RSM), Fuel (2020) 119528.
[34] P. Adewale, L.N. Vithanage, L. Christopher, Optimization of enzyme-catalyzed biodiesel production from crude tall oil using Taguchi method, Energy Conversion and Management 154 (2017) 81-91.
[35] M. Kadir Yesilyurt, C. Cesur, Biodiesel synthesis from Styrax officinalis L. seed oil as a novel and potential non-edible feedstock: A parametric optimization study through the Taguchi technique, Fuel 265 (2020) 117025.
[36] A.B. Fadhil, K.M. Ahmed, M.M. Dheyab, Silybum marianum L. seed oil: A novel feedstock for biodiesel production, Arabian Journal of Chemistry 10 (2017) S683-S690.
[37] K.V. Avramidou, F. Zaccheria, S.A. Karakoulia, K.S. Triantafyllidis, N. Ravasio, Esterification of free fatty acids using acidic metal oxides and supported polyoxometalate (POM) catalysts, Molecular Catalysis 439 (2017) 60-71.
[38] M. Helmi, K. Tahvildari, The effect of changing the concentration of loaded KOH to a zeolite heterogeneous catalyst activity in biodiesel production by electrolysis, International Journal of Advanced Biotechnology and Research (IJBR) 7 (2016) 79-85.
[39] Y.H. Tan, M.O. Abdullah, C. Nolasco-Hipolito, N.S. Ahmad Zauzi, Application of RSM and Taguchi methods for optimizing the transesterification of waste cooking oil catalyzed by solid ostrich and chicken-eggshell derived CaO, Renewable Energy 114 (2017) 437-447.
[40] S.H. Dhawane, A.P. Bora, T. Kumar, G. Halder, Parametric optimization of biodiesel synthesis from rubber seed oil using iron doped carbon catalyst by Taguchi approach, Renewable Energy 105 (2017) 616-624.
[41] G. De Bhowmick, R. Sen, A.K. Sarmah, Analysis of growth and intracellular product synthesis dynamics of a microalga cultivated in wastewater cocktail as medium, Biochemical Engineering Journal 149 (2019) 107253.
[42] S.H. Dhawane, B. Karmakar, S. Ghosh, G. Halder, Parametric optimisation of biodiesel synthesis from waste cooking oil via Taguchi approach, Journal of Environmental Chemical Engineering 6 (2018) 3971-3980.

[43] V. Ayhan, Ç. Çangal, İ. Cesur, A. Çoban, G. Ergen, Y. Çay, A. Kolip, İ. Özsert, Optimization of the factors affecting performance and emissions in a diesel engine using biodiesel and EGR with Taguchi method, Fuel 261 (2020) 116371.
[44] B. Karmakar, B. Ghosh, S. Samanta, G. Halder, Sulfonated catalytic esterification of Madhuca indica oil using waste Delonix regia: L16 Taguchi optimization and kinetics, Sustainable Energy Technologies and Assessments 37 (2020) 100568.
[45] S.H. Dhawane, T. Kumar, G. Halder, Biodiesel synthesis from Hevea brasiliensis oil employing carbon supported heterogeneous catalyst: Optimization by Taguchi method, Renewable Energy 89 (2016) 506-514.
[46] A. Marwaha, P. Rosha, S.K. Mohapatra, S.K. Mahla, A. Dhir, Biodiesel production from Terminalia bellerica using eggshell-based green catalyst: An optimization study with response surface methodology, Energy Reports 5 (2019) 1580-1588.
[47] B. Khodadadi, M. Bordbar, A. Yeganeh-Faal, M. Nasrollahzadeh, Green synthesis of Ag nanoparticles/clinoptilolite using Vaccinium macrocarpon fruit extract and its excellent catalytic activity for reduction of organic dyes, Journal of Alloys and Compounds 719 (2017) 82-88.
[48] j. mahmoudi, m. Rahimi, Studies on optimization of efficient parameters for removal of lead from aqueous solutions by natural zeolite as a low-cost adsorbent using response surface methodology, Advances in Environmental Technology 3 (2017) 99-108.
[49] A. Mohseni-Bandpi, T.J. Al-Musawi, E. Ghahramani, M. Zarrabi, S. Mohebi, S.A. Vahed, Improvement of zeolite adsorption capacity for cephalexin by coating with magnetic Fe3O4 nanoparticles, Journal of Molecular Liquids 218 (2016) 615-624.
[50] A. Khodadadi Dizaji, H.R. Mortaheb, B. Mokhtarani, Preparation of supported catalyst by adsorption of polyoxometalate on graphene oxide/reduced graphene oxide, Materials Chemistry and Physics 199 (2017) 424-434.
[51] A. Khodadadi Dizaji, H.R. Mortaheb, B. Mokhtarani, Extractive-Catalytic Oxidative Desulfurization with Graphene Oxide-Based Heteropolyacid Catalysts: Investigation of Affective Parameters and Kinetic Modeling, Catalysis Letters 149 (2019) 259-271.

[52] Y. Kim, S. Shanmugam, Polyoxometalate–Reduced Graphene Oxide Hybrid Catalyst: Synthesis, Structure, and Electrochemical Properties, ACS Applied Materials & Interfaces 5 (2013) 12197-12204.

[53] L. Kubelková, B. Wichterlová, P. Jacobs, N. Jaeger, Zeolite Chemistry and Catalysis, Elsevier1991.

[54] N. Safajoo, B.B.F. Mirjalili, A. Bamoniri, Fe 3 O 4@ nano-cellulose/Cu (ii): a bio-based and magnetically recoverable nano-catalyst for the synthesis of 4 H-pyrimido [2, 1-b] benzothiazole derivatives, RSC advances 9 (2019) 1278-1283.

[55] M.H. Firouzjaee, M. Taghizadeh, Optimization of Process Variables for Biodiesel Production Using the Nanomagnetic Catalyst CaO/NaY-Fe3O4, Chemical Engineering & Technology 40 (2017) 1140-1148.

[56] A.P. Bora, S.H. Dhawane, K. Anupam, G. Halder, Biodiesel synthesis from Mesua ferrea oil using waste shell derived carbon catalyst, Renewable Energy 121 (2018) 195-204.

[57] A. E2881-18, Standard Test Method for Extraction and Derivatization of Vegetable Oils and Fats from Fire Debris and Liquid Samples with Analysis by Gas Chromatography-Mass Spectrometry, ASTM International West Conshohocken (2018).

[58] A. Talebian-Kiakalaieh, N.A.S. Amin, A. Zarei, I. Noshadi, Transesterification of waste cooking oil by heteropoly acid (HPA) catalyst: Optimization and kinetic model, Applied Energy 102 (2013) 283-292.

[59] H. Pan, H. Li, H. Zhang, A. Wang, D. Jin, S. Yang, Effective production of biodiesel from non-edible oil using facile synthesis of imidazolium salts-based Brønsted-Lewis solid acid and co-solvent, Energy Conversion and Management 166 (2018) 534-544.

[60] A.B. Sahabdheen, A. Arivarasu, Synthesis and characterization of reusable heteropoly acid nanoparticles for one step biodiesel production from high acid value waste cooking oil – Performance and emission studies, Materials Today: Proceedings 22 (2020) 383-392.

[61] A.C.M. Loy, A.T. Quitain, M.K. Lam, S. Yusup, M. Sasaki, T. Kida, Development of high microwave-absorptive bifunctional graphene oxide-based catalyst for biodiesel production, Energy Conversion and Management 180 (2019) 1013-1025.

[62] R. Malhotra, A. Ali, 5-Na/ZnO doped mesoporous silica as reusable solid catalyst for biodiesel production via transesterification of virgin cottonseed oil, Renewable Energy 133 (2019) 606-619.
[63] M. Rosset, O.W. Perez-Lopez, FTIR spectroscopy analysis for monitoring biodiesel production by heterogeneous catalyst, Vibrational Spectroscopy 105 (2019) 102990.
[64] N.M. Niza, K.T. Tan, Z. Ahmad, K.T. Lee, Comparison and optimisation of biodiesel production from Jatropha curcas oil using supercritical methyl acetate and methanol, Chemical papers 65 (2011) 721-729.
[65] L. Fereidooni, M. Mehrpooya, Experimental assessment of electrolysis method in production of biodiesel from waste cooking oil using zeolite/chitosan catalyst with a focus on waste biorefinery, Energy Conversion and Management 147 (2017) 145-154.
[66] E.P. Favvas, C.G. Tsanaktsidis, A.A. Sapalidis, G.T. Tzilantonis, S.K. Papageorgiou, A.C. Mitropoulos, Clinoptilolite, a natural zeolite material: Structural characterization and performance evaluation on its dehydration properties of hydrocarbon-based fuels, Microporous and Mesoporous Materials 225 (2016) 385-391.
[67] C.G. Tsanaktsidis, S.G. Christidis, E.P. Favvas, A novel method for improving the physicochemical properties of diesel and jet fuel using polyaspartate polymer additives, Fuel 104 (2013) 155-162.
[68] Y. Huang, Y. Li, X. Han, J. Zhang, K. Luo, S. Yang, J. Wang, Investigation on fuel properties and engine performance of the extraction phase liquid of bio-oil/biodiesel blends, Renewable Energy 147 (2020) 1990-2002.
[69] M. Tariq, S. Ali, F. Ahmad, M. Ahmad, M. Zafar, N. Khalid, M.A. Khan, Identification, FT-IR, NMR (1H and 13C) and GC/MS studies of fatty acid methyl esters in biodiesel from rocket seed oil, Fuel Processing Technology 92 (2011) 336-341.
[70] M. Guillén, P. Uriarte, Study by 1H NMR spectroscopy of the evolution of extra virgin olive oil composition submitted to frying temperature in an industrial fryer for a prolonged period of time, Food Chemistry 134 (2012) 162-172.
[71] N.A. Portela, E.C.S. Oliveira, A.C. Neto, R.R.T. Rodrigues, S.R.C. Silva, E.V.R. Castro, P.R. Filgueiras, Quantification of biodiesel in petroleum diesel by 1H NMR: Evaluation of univariate and multivariate approaches, Fuel 166 (2016) 12-18.

[72] D. Papargyriou, E. Broumidis, M. de Vere-Tucker, S. Gavrielides, P. Hilditch, J.T.S. Irvine, A.D. Bonaccorso, Investigation of solid base catalysts for biodiesel production from fish oil, Renewable Energy 139 (2019) 661-669.
[73] C.N. Ibeto, C.O.B. Okoye, A.U. Ofoefule, Comparative study of the physicochemical characterization of some oils as potential feedstock for biodiesel production, ISRN Renewable Energy (2012).
[74] M. Da Silva, M. Teixeira, An unexpected behavior of H 3 PMo 12 O 40 heteropolyacid catalyst on the biphasic hydrolysis of vegetable oils, RSC Advances 7 (2017) 8192-8199.